Article

The Role of the Catalyst on the Reactivity and Mechanism in the Diels–Alder Cycloaddition Step of the Povarov Reaction for the Synthesis of a Biological Active Quinoline Derivative: Experimental and Theoretical Investigations

Soumia Lamri [1], Affaf Heddam [1], Meriem Kara [1], Wassila Yahia [2] and Abdelmalek Khorief Nacereddine [1,*]

[1]   Laboratory of Physical Chemistry and Biology of Materials, Department of Physics and Chemistry, Higher Normal School of Technological Education-Skikda, Azzaba, Skikda 21300, Algeria; sousou2014888@gmail.com (S.L.); takwaafaf@gmail.com (A.H.); meriemkara368@gmail.com (M.K.)

[2]   Department of Chemistry, Faculty of Sciences, University August 20 1955 Skikda, BP 26, Skikda 21000, Algeria; w_bio2005@yahoo.fr

*   Correspondence: malek_khorief@yahoo.com or a.khorief@enset-skikda.dz

Abstract: An experimental and theoretical study of the reactivity and mechanism of the non-catalyzed and catalyzed Povarov reaction for the preparation of a 4-ethoxy-2,3,4,4a-tetrahydro-2-phenylquinoline as a biological active quinoline derivative has been performed. The optimization of experimental conditions indicate that the use of a catalyst, namely Lewis acid with an electron-releasing group, creates the best experimental conditions for this kind of reaction. The chemical structure was characterized by the usual spectroscopic methods. The prepared quinoline derivative has been also tested in vitro for antibacterial activity, which displays moderate inhibitory activity against both *Escherichia coli* and *Staphylococcus aureus*. The antioxidant activity was investigated in vitro by evaluating their reaction with 1,1-diphenyl-2-picrylhydrazyl DPPH radical, which reveals high reactivity. The computational study was performed on the Diels–Alder step of the Povarov reaction using a B3LYP/6-31G(d,p) level of theory. The conceptual DFT reactivity indices explain well the reactivity and the *meta* regioselectivity experimentally observed. Both catalysts enhance the reactivity of the imine, favoring the formation of the *meta* regioisomers with a low activation energy, and they change the mechanism to highly synchronous for the Lewis acid and to stepwise for the Brønsted acid. The reaction of imine with allyl alcohol does not give any product, which requires high activation energy.

Keywords: quinoline; Povarov; antibacterial; antioxidant; DFT; CDFT; mechanism; [4+2] cycloaddition

1. Introduction

The nitrogenous heterocycles are important biologically active molecules and are considered as scaffolds for discovering new pharmaceutical products [1]. Quinolines and their derivatives represent an important class of nitrogenous heterocycles, which attract the attention of chemists, because the 1,2,3,4-tetrahydroquinoline structure is located in tremendous bioactive compounds [2–4]. Indeed, quinoline derivatives have displayed various applications such as anticancer [5], antimycobacterial [6], antimicrobial [7], anticonvulsant [8], analgesic and anti-inflammatory activity [9], and cardiovascular agent [10]. Today, many methods have been discovered in order to prepare tetrahydroquinoline derivatives [11,12]. The Diels–Alder (DA) reaction is an important reaction for the synthesis of carbocyclic and heterocyclic molecules [13]. The aza-Diels–Alder reaction between N-aryl imines and nucleophilic olefins was widely used for the synthesis of tetrahydroquinoline derivatives using an appropriate catalyst.Today, a considerable number of different Lewis acids were engagedas catalysts in an aza-Diels–Alder reaction between N-aryl imines and nucleophilic

olefins for the goal of preparing new tetrahydroquinoline derivatives [14–16]. Moreover, the availability of catalysts and their efficiency remains a major problem in aza Diels–Alder reactions. Among the reactions of aza Diels–Alder, the Povarov reaction [17] is characterized by an inverse electrondemand, and it occurs between substituted aromatic imines and electron-rich olefins, leading to a rapid formation of tetrahydroquinolines. Among the used catalysts in this reaction are the protic or Lewis acids, using aromatic imines and olefins or with multi-component reaction from starting reagents, aniline, aldehyde, and olefin [18–25].

As part of our ongoing efforts in the field of cycloaddition (CA) reactions with catalysts for the synthesis of novel polyfunctionalized heterocycles [26–30], herein, we report, for the first time, an experimental study for the synthesis of a quinoline derivativeviathe Povarov reaction between imine (generated from benzaldehyde and aniline) and different substituted ethylenes. Then, the obtained products have undergone a spectral analysis and an evaluation of their antibacterial and antioxidant biological activities. For the second time, we report deep computational investigations of the reactivity and selectivity of this reaction.

2. Results and Discussion

The present study has been divided into two dependent parts. Firstly, we have performed the synthesis of quinoline derivative **5** using a Povarov cycloaddition reaction between the commercially alkene **1** and the prepared imine **2**, without and with different types of catalysts. Secondly, the selectivity and the mechanism of the experimentally Povarov reaction were studied computationally using Density Functional Theory (DFT) methods through different theoretical theorems and models, namely, transition state theory [31] and conceptual DFT (CDFT) reactivity indices [32,33].

2.1. Synthetic Study

2.1.1. Imine

Imines are useful building blocks thathave been widely used for the synthesis of nitrogenous bioactive heterocyclic materials and are used in industrial and academic fields [34]. The imines that have an alkyl or aryl group linked to the nitrogen atom are named Schiff bases [35]. Those are generallyobtained from the condensation reaction between a primary amine and a carbonyl compound. The name Schiff base is related to Schiff, who discovered them [36]. These compounds are attractive due to their highly coordinated behaviors as ligands [37].

The benzylidenebenzenamine (imine **2**) was easily obtained using condensation between benzaldehyde and aniline in refluxing ethanol and then in room temperature according to the protocol described in the literature (Scheme S1 in SI) [36].
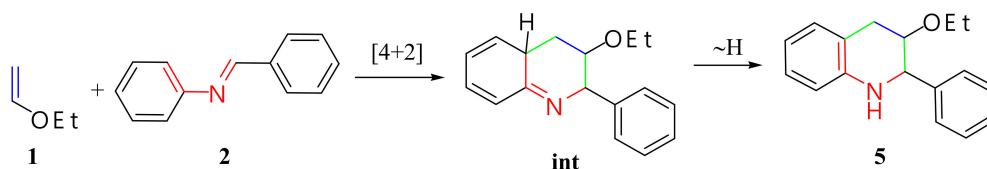
In ethanol, at the temperature of the refluxing solvent, the reaction with an equimolecular amount of benzaldehyde and aniline, with respect to the substrates, gave 60% yield.

The obtaining of the desired product is confirmed by its melting point, which was found to be 54 °C, which was similar to the theoretical (from 52 to 54 °C).

2.1.2. Quinoline Derivative

The preparation of the quinoline derivative is based on the condensation between the imine **2** prepared previously and the commercially available alkene **1** according to the Povarov experimental protocol [17] (Scheme 1). Alternatively, there can be a multi-component reaction whereaniline, benzaldehyde, and electron-rich alkene (alkene **1**) react simultaneously, in which the imine is generated in situand then reacts with alkene **1** [16,18,38,39]. The pilot reaction was carried out with different catalysts using the imine **2** and vinyl ethyl ether **1** as a promoting system to find the best reaction catalyst, as described in Table 1.In the case of the Brønsted acid catalyst experiment, the imines are generated in situ from the condensation reaction between aldehyde and aromatic amines. After that, the generated imines react directly with electron-rich alkene to produce the *meta*-regioisomer of quinoline

5 in a single operation without going through the preparation of imines. After filtration, the filtrates are concentrated to give almost pure quinoline derivative **5** in moderate to good yields (see Table 1).

Scheme 1. Synthesis of quinoline derivative **5** via [4+2] cycloaddition between imine **2** and electron-rich ethylene **1**.

Table 1. Conditions optimization of the synthesis of quinoline derivative **5**.

Entry	Solvent	Catalyst	Temperature	Time (h)	Yield (%)
1	diethylether	none	rt	48	no reaction
2	diethylether	AlCl$_3$	rt	48	79
3	ethanol	HCl	rt	48	60
4	ethanol/acetonitrile	CH$_3$COOH	rt	48	30

From Table 1, we can notice that except for entry 1 (absence of catalyst), in all other cases, whether it be the used catalyst, Lewis acid, or Brønsted acid, the Povarov reaction proceeded successfully to give the meta regioisomer of quinoline derivative **5** as a yellow–brown oil. In addition, the remarkable notice is that the best yield is obtained with the use of the AlCl$_3$ catalyst (60%), indicatingthat the Lewis acid catalyst is the best catalyst for this reaction type. The low yield obtained with the use of acetic acid (30%) may be attributed to its marginally acidic character, which does not give the necessary catalyst amount for this reaction.

The reaction between imine **2** and allyl alcohol does not produce any product, despite we have used different catalysts.

2.2. Biological Activity

In this part, the biological activity of the obtained quinoline derivative, namely the antioxidant and the antibacterial activity, were evaluated.

2.2.1. Antibacterial Activity

The synthesized quinoline derivative **5** was screened for its antibacterial activity against six different types of strains of bacteria, including Gram-negative and Gram-positive using DMSO solvent and the antibiogram method. The antibiogram analysis against bacteria was performed according to the method reported in the literature [40]. The obtained results of antibacterial activity are depicted in Figure 1 and Table 2.
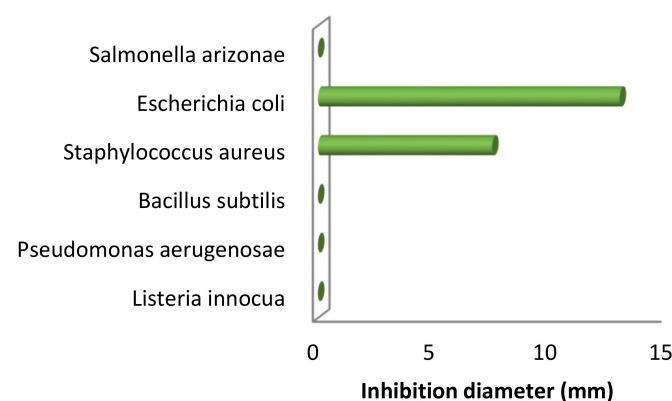

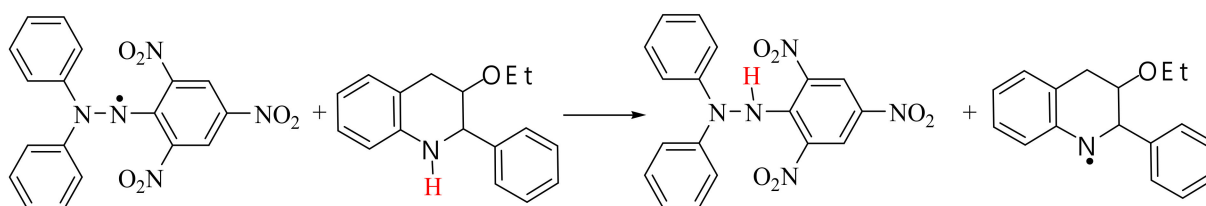**Figure 1.** Antibacterial activity versus type of bacteria.

Table 2. Antibacterial activity of quinoline **5**.

Type of Bacteria	Inhibition Diameter (mm)
Listeria innocua CLIP 74915	-
Pseudomonas aerugenosae ATCC 2592	-
Bacillus subtilis ATCC 26023	-
Staphylococcus aureus ATCC 29213	7.5
Escherichiacoli ATCC 25922	13
Salmonella arizonae CIP 81-3	-

Through the obtained results, we can conclude that the prepared quinoline derivative **5** has a moderate antibacterial activity against *Staphylococcus aureus* and *Escherichia coli*.

2.2.2. Antioxidant Activity

In this part, we turned our attention to the antioxidant activity of quinoline derivative **5**. Antioxidants are important compounds that arewidely known for their high reactivity against free radicals causing various diseases, namely, cancer, hyperuricemia, cell aging, and cardiovascular problems [41]. In order to estimate the antioxidant activity of the prepared quinoline (**5**) in vitro, the commercially available 1,1-diphenyl-2-picrylhydrazyl radical (DPPH·) was engaged in reaction with the *meta* regioisomer of quinoline **5**. This type of analysis was widely used in the case of compounds with SH-, NH-, and OH groups [42]. The mechanism of this reaction is depicted in Scheme 2. The DPPH radical scavenging activity of quinoline **5** was estimated according to changes of DPPH color after 10 min incubation in the dark and at room temperature [43].

Scheme 2. Reaction between DPPH and quinoline derivative **5**.

According to the results, in which the color changes from violet (color attributed to the DPPH radical) to yellow, compound **5** has reacted with DPPH, indicatingthat ithas a significant inhibitory effect against the DPPH radical.

2.3. Computational Study

2.3.1. Methods and Models

The computations were performed using Gaussian 09 suite software [44]. The structures associated with the studied Povarov reactions have been optimized using the B3LYP functional together with the 6-31G(d,p) basis set [45–47]. The optimized structures have been subjected to a frequency calculation to confirm obtaining a minimum or a transition state (TS), in which the TS is characterized by one imaginary frequency. The natural bond orbital (NBO) method was used to analyze the electronic structures of the TSs [48]. The global electrophilicity index ω [49] can be calculated using the following equation, $\omega = \frac{\mu^2}{2\eta}$, in which μ is the electronic chemical potential and η is the chemical hardness. Those are calculated using the energies of the frontier molecular orbitals, Highest Occupied Molecular Orbital (HOMO) and Lowest Unoccupied Molecular Orbital (LUMO), ε_H and ε_L, through the following equations: $\mu \approx (\varepsilon_H + \varepsilon_L)/2$ and $\eta \approx (\varepsilon_L - \varepsilon_H)$, respectively [50]. The nucleophilicity index, [51] N, which is calculated basing on the HOMO energies obtained within the Kohn–Sham scheme [52], is given as $N = \varepsilon_{HOMO\,(Nu)} - \varepsilon_{HOMO(TCE)}$, where tetracyanoethylene (TCE) was taken as a reference because it has the lowest HOMO energy in a vast series of molecules that has been studied in polar organic reactions. The electrophilic

P_k^+ and nucleophilic P_k^- Parr functions [53] were obtained through the analysis of the Mulliken atomic spin densities (ASD) of the corresponding radical anion and radical cation by single-point energy calculations through the optimized gas phase neutral geometries.

2.3.2. Analysis of Reactivity Indices Derived from Conceptual DFT

Global Indices

The calculated Global Electron Density Transfer (GEDT) values at the transition states [54] were used to analyze the polarity of the studied reaction through the electron density transfer from the nucleophile fragment toward the electrophile fragment, in which the non-polar reaction is characterized by a low value of the GEDT. A tremendous number of studies can be found in the literature, indicating the relationship between the nature of the reactants and the polar character of the reactions [55–59]. Thus, the reactivity of the reagents as well as the feasibility of the reaction can be studied through these indices [33,60]. The global reactivity indices of alkene **1**, imine **2**, imine:H$^+$ complex **3** and imine: AlCl$_3$ complex **4** are calculated and given in Table 3, while that of allyl alcohol is given in Table S1 in the Supplementary Material.

Table 3. Global conceptual DFT (CDFT) reactivity properties calculated, in eV, of Alkene **1**, imines **2**, **3**, and **4**.

	HOMO	LUMO	μ	η	ω	N
Alkene **1**	−5.89	1.07	−2.41	6.95	0.42	3.23
Imine **2**	−5.91	−1.57	−3.74	4.34	1.61	3.21
Imine **3**	−10.30	−6.73	−8.52	3.57	10.16	−1.18
Imine **4**	−7.15	−2.90	−5.03	4.25	2.97	1.97

The electronic chemical potential of alkene **1**, μ = −2.41 eV is higher than that of imine **2** and its complexes forms, imines **3** and **4**. Thereby, during these reactions, the GEDT will take place from alkene **1** toward imines **2**, **3**, and **4**, in accordance with the calculated GEDT values. On the other hand, the electrophilicity and nucleophilicity indices of alkene 1 are ω= 0.42 and N = 3.23 eV, indicating that it is a marginal electrophile and a strong nucleophile based on the electrophilicity [61] and nucleophilicity scales [62]. Otherwise, the electrophilicity and nucleophilicity indices of imine **2** are ω= 1.61 and N =3.21 eV. Thereby, alkene **1** and imine **2** poss the same reactivity behaviors, accounting that the reaction between them requires high activation energy, which is in accordance with what has been seen experimentally.For the case with the addition of a catalyst, both catalysts prove to enhance dramatically the electrophilicity power and decrease the nucleophilicity of the imine, especially Brønsted acid. Therefore, in all cases, alkene **1** will react as a strong nucleophile, whereas imine **2** will react as a marginal electrophile, and imines **3** and **4** will react as strong electrophiles. Consequently, with uses of acid catalysts, especially Brønsted acid, these cycloaddition reactions present relatively low activation energy and high values of GEDT (see later).

For the allyl alcohol, it does not have a strong nucleophilic character (N = 2.44 eV), which is less than that of imine **2**; that may be due to the absence of an electron realizing group such as the case of vinyl ethyl ether (alkene **1**).

Local Indices

Figure 2 illustrates the three-dimensional atomic spin densities (ASD) of the radical cation alkene **1$^+$**, while the radical anions imines **2$^-$**, **3$^-$**, and **4$^-$**, as well as the values of nucleophilic Parr functions local indices of alkene **1** and the electrophilic Parr functions local indices of imines **2**, **3**, and **4**, and for that of allyl alcohol, are given in Figure S1 in Supplementary Material. From Figure 1, the higher electrophilic Parr function local index of all imines is concentrated at the carbon atom C4 of imines **2**, **3**, and **4** (for atom numbering, see Scheme 4), with a value of P_k^+ = 0.270, 0.484, and 0.542, respectively. In contrast, for the nucleophilic P_k^- Parr function local indices of alkene 1, we can clearly see at the C5=C6

reactive region that C5 has the higher value of local indices ($P_k^- = 0.57$), which reveals that it is the most nucleophilic center in this nucleophilic reagent. In polar reactions, the favorable interaction between reactive centers will occur between the most electrophilic center of the electrophile and the most nucleophilic center of the nucleophile [63]. Therefore, the studied cycloaddition reaction step will form only the *meta* regioisomers, which is inaccordance with experimental findings (see above) and the analysis of energy profiles (see later).
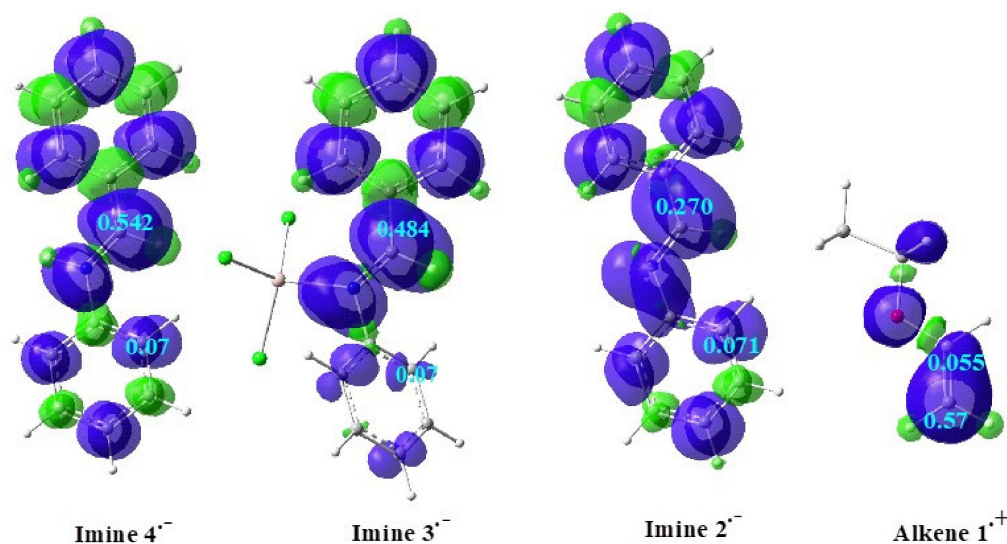

Figure 2. Maps of the atomic spin densities (ASD) of the radical anions of imines **2**, **3**, and **4** with the radical cations of alkene **1** with isovalue = 0.008 together with the nucleophilic and electrophilic indices.
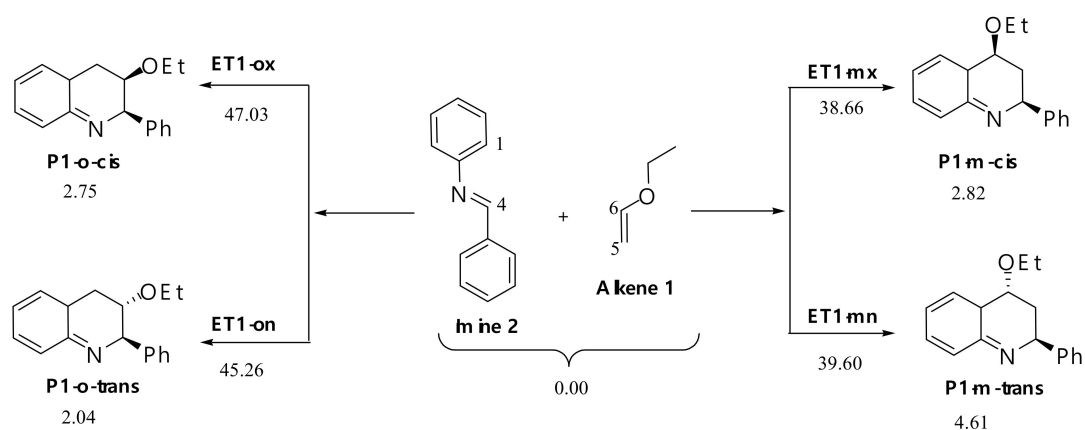
2.3.3. Energetic Aspects

The transition state theory [31] is the only method that enables us to study the regioselectivity (*ortho*/*meta*) together with the stereoselectivity (*endo*/*exo*), where, based on the comparison between the activation energy of the possible transition states, we can identify the kinetic product, that is the compound thatformed in high speed(the product has the lowest activation energy). On the other hand, based on the energy values of the products, we can determine the nature of the reaction (reversible or irreversible). Moreover, the comparison between the energy of the products enables us to know the most stable compound, i.e., the thermodynamic product.

Non-Catalyzed Reaction

The intrinsic reaction coordinates (IRC) paths indicated that the non-catalyzed Povarov reaction of imine **2** with alkene **1** takes place through a one-step mechanism, and because alkene **1** and imine **2** have asymmetric structures, the reaction between them could take place along four possible reactive pathways, which are two reagioisomeric reactive channels, namely, ortho and meta, in two stereoisomeric approaches, endo and exo (see Scheme 3). Accordingly, for this CA reaction, we have located and characterized the reagents, four TSs, and the corresponding four cycloadducts (CAs). The relative energies of the stationery points of the non-catalyzed Povarov reaction between alkene 1 and imine 2 in gas phase are given in Scheme 3, while the total ones are collected in Table S1 in the Supplementary Material.

From an analysis of activation energies, we can notice that the meta-regioisomers is more kinetically favored than the ortho ones by about 6.60 kcalmol^{-1}, in which the meta-exo approach is slightly more favored than the meta-endo one by 0.94 kcalmol^{-1}.On the other hand, all cycloadducts are less stable than the separated reagents, alkene **1** and imine **2**. Therefore, those pathways are unfavorable both kinetically and thermodynamically, explaining there being no observed reaction in the experimental part.

Scheme 3. The pathways involved in the Povarov reaction of alkene **1** with imine **2** together with the values of relative energies.

The optimized geometries of the TSs associated with the non-catalyzed Povarov reaction between alkene **1** and imine **2** are given in Figure 3. At the meta TSs, the distances C1 ... C6, and C4 ... C5 single new forming bonds are 1.80 and 2.64 Å at **TS1mx** and 1.85 and 2.53 Å at **TS1mn**, respectively, while at the *ortho* TSs, the distances between C1 ... C5 and C4 ... C6 of the corresponding new single bonds are 2.39 and 1.94 Å at **TS1ox** and 2.16 and 2.11 Å at **TS1on**. Therefore, except for the formation of **TS1ox** that is slightly synchronous, the new C–C single bonds at the other TSs take place through relatively asynchronous bond formation processes, in which the formation of the C1–C6 single bond is more advanced than the C4–C5 one at the *meta* TSs, while for **TS1-ox**, the formation of the C1–C5 single bond is more advanced than the C4–C6 one.
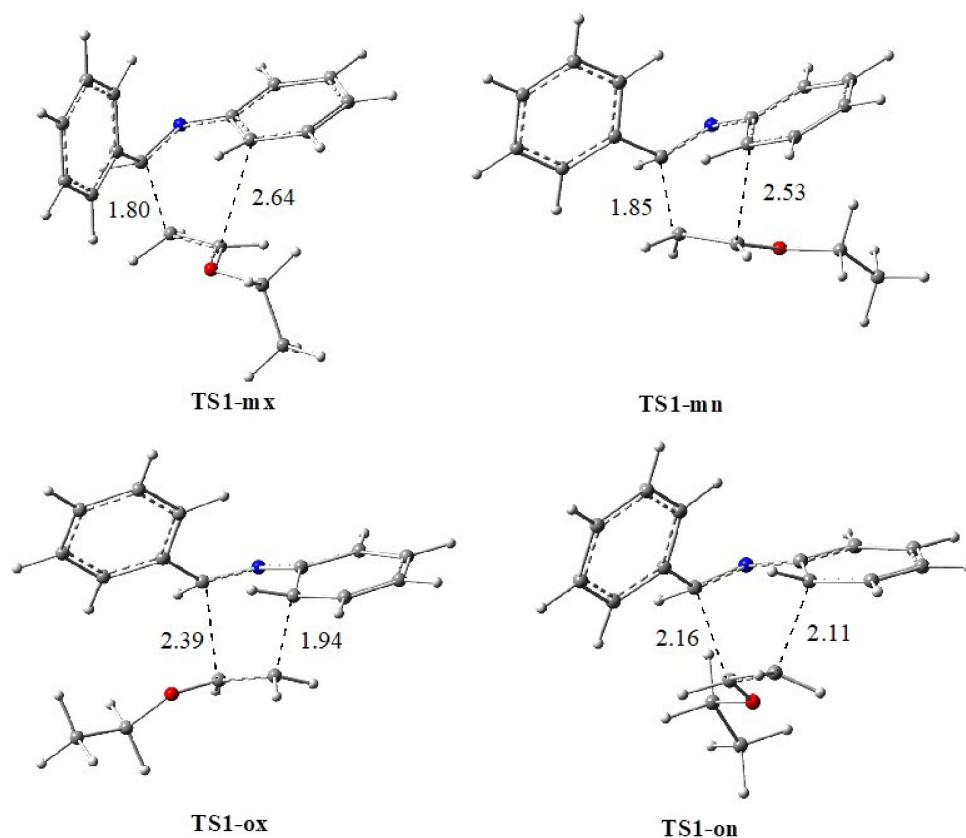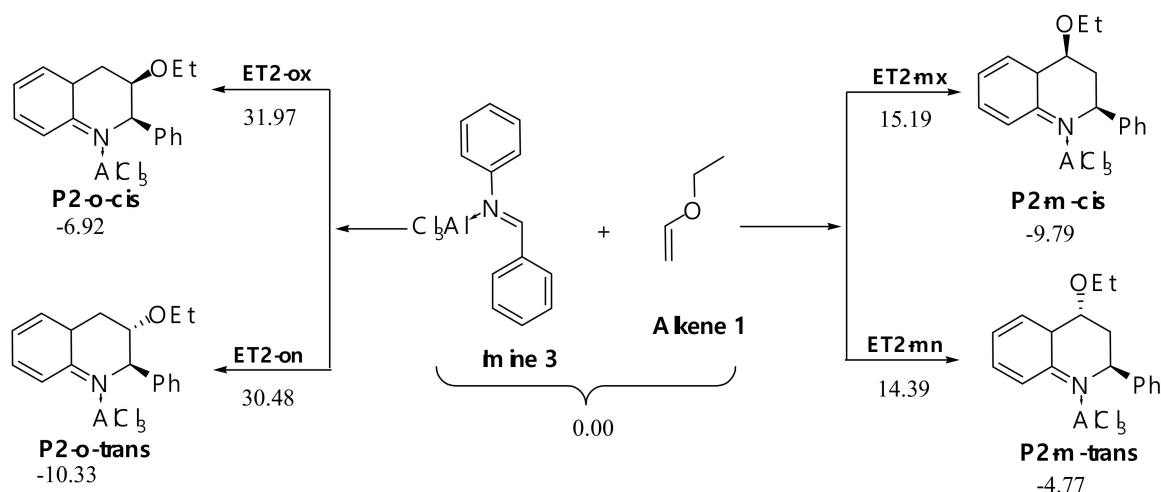

Figure 3. Optimized structures of the transition state (TSs) associated with the reaction between imine **2** and alkene **1**, together with lengths of the new forming bonds.

The electronic nature of the non-catalyzed Povarov reaction of alkene **1** with imine **2** was evaluated by calculating the value of GEDT [54] at all transition states. The values of the GEDT computed at the alkene **1** moiety of the TSs are 0.13e at **TS1-mn**, 0.12e at **TS1-mx**, 0.05e at **TS1-on**, and 0.06e at **TS1-ox**. These low values indicate that the non-catalyzed Povarov reaction of alkene **1** with imine **2** has a low polar character, which is in agreement with the analysis of the global reactivity indices and with the obtained high activation energy for this reaction.

AlCl₃ Catalyzed Reaction

Coordination of the nitrogen atom (C=N) of imine **2** with an AlCl₃ catalyst forms complex imine **3**, which notably increases its electrophilicity and enhances its reactivity toward electron-rich alkene such as alkene **2** (see above in Section 2.3.2). Analysis of the IRC paths of the AlCl₃ catalyzed CA reactions of the imine **3** complex with alkene **1** indicates that this CA reaction takes place through a one-step mechanism. Thereby, always, this CA reaction can follow four reactive pathways; therefore, we will study four possible CAs with four corresponding TSs (Scheme 4). The structure of the corresponding transition states for this reaction as well as the lengths of the new forming bonds are shown in Figure 4. The relative energies of the reactants, CAs, and TSs of the AlCl₃ catalyzed cycloaddition reaction between the imine **3** complex and alkene **1** were calculated and then given in Scheme 5, while the total ones are collected in Table S2 in Supplementary Material.

Scheme 4. The pathways involved in the Povarov reaction of alkene **1** with AlCl₃:imine complex **3**, together with the values of the relative energies (in kcal/mol).

Through the results recorded in Scheme 4, we notice that the CA meta-endo is the kinetic preferred path (Ea = 14.39 kcal/mol). In addition, this approach is more stable than the meta-endo one by 16.09 kcal/mol, which indicates that this reaction leads to the formation of meta regioisomers, which is in agreement with the CDFT local reactivity indices analysis. We also note that this reaction requires small activation energy in comparison with the non-catalyzed reaction, meaning that the Lewis acid catalyst activates the reaction despite any further activation by heating or light rays, and this explains the occurrence of the reaction experimentally unlike the previous reaction without a catalyst.
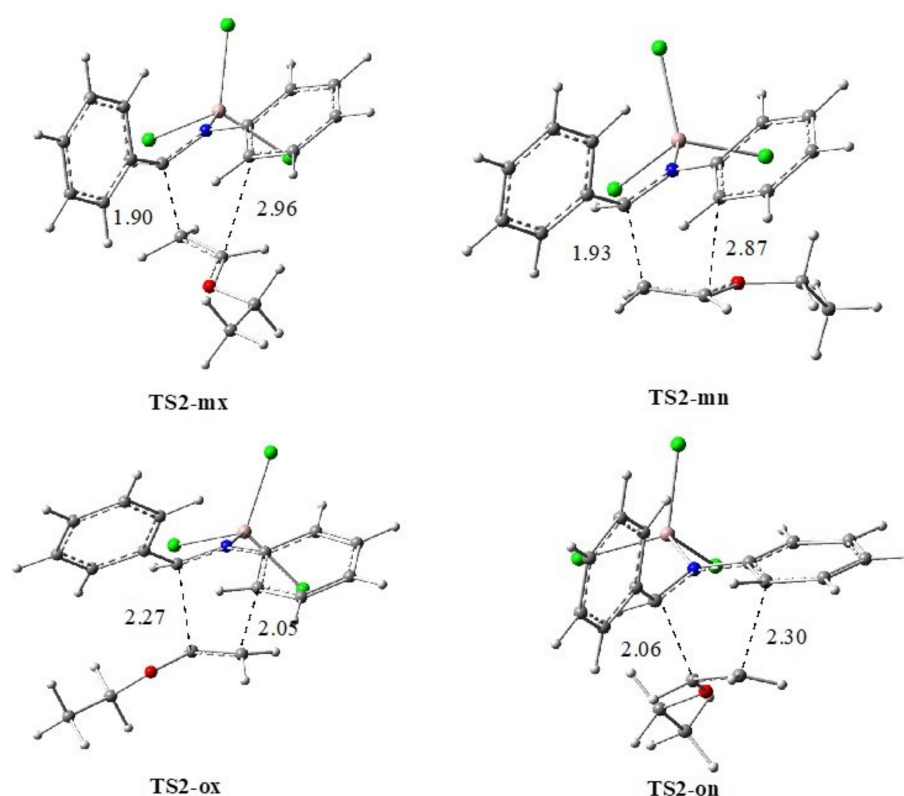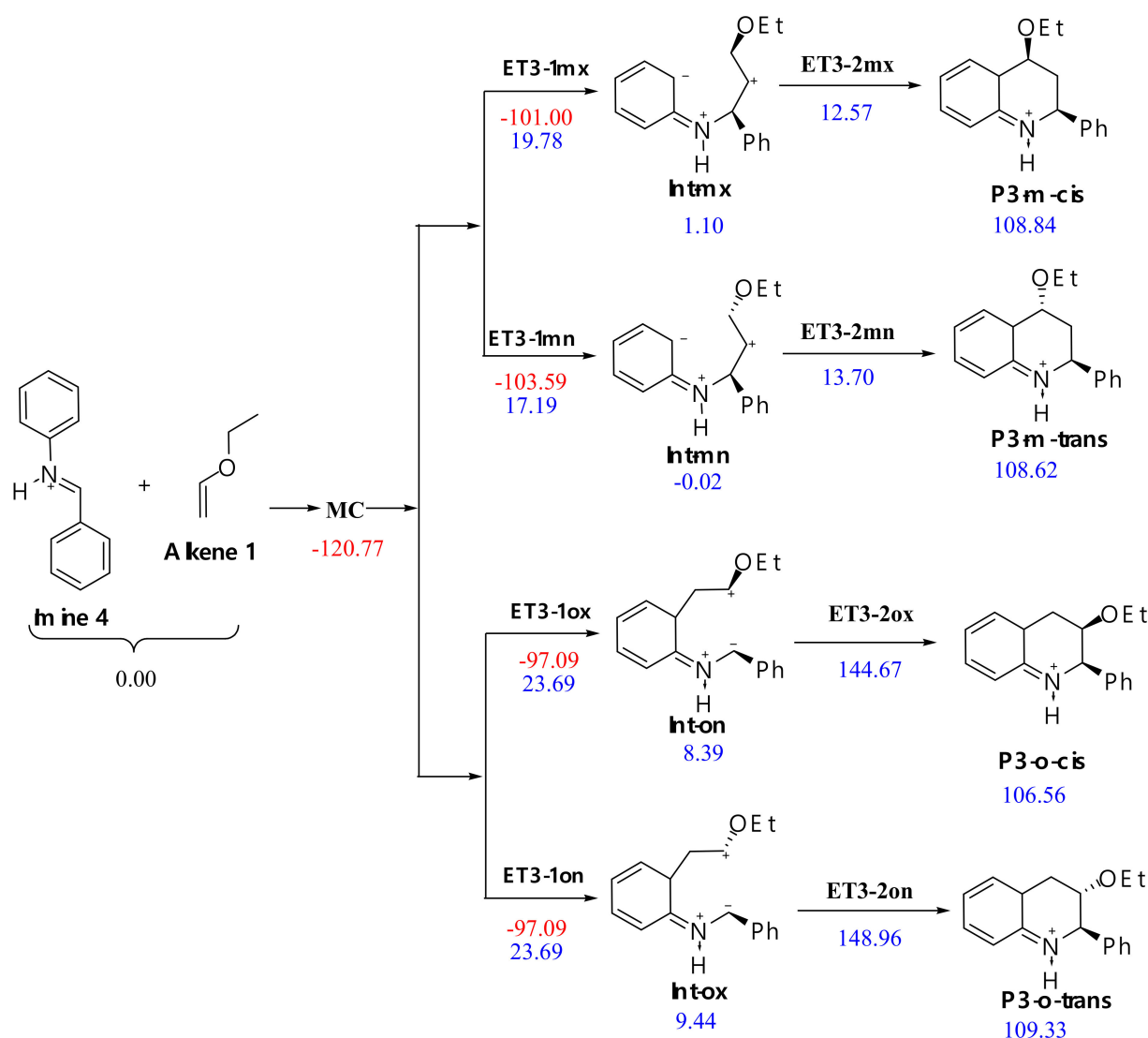
Figure 4. Optimized structures of the TSs associated with the catalyzed reaction between imine:AlCl$_3$ complex **3** and alkene **1**, together with lengths of the new forming bonds.

From Figure 4 and by a comparison between the lengths of the new formed bonds at the TSs, we remarked that all the reactive pathways proceed via an asynchronous mechanism with the C−C bond in which the non-substituted carbon of alkene **1** is slightly more advanced than the other C−C one. In addition, the preferred reactive pathways **TS2-mx** and **TS2-mn** are more asynchronous than the ortho ones. This indicates that the LA catalyst changes the mechanism nature of these processes. Indeed, it become highly asynchronous, since the difference between the lengths of the new forming bonds is 1.06 and 0.94Å for **TS2mn** and **TS2mx**, respectively.

The values of GEDT, which its flux takes place from alkene **1** to the electrophilically activated AlCl$_3$:imine complex **3**, are 0.419e (**TS2mx**), 0.458e (**TS2mn**), 0.238e (**TS2ox**), and 0.259e (**TS2on**). The GEDT found in these TSs accounts for the polar character of this LA catalyzed CA reaction. Therefore, the LA catalyst increases the polar character of these CA reactions, explaining the decrease of the activation energies of these processes [64].

H$^+$ Catalyzed Reaction

In this reaction, also, the two reactants follow four possible reactive pathways; in addition, the IRC paths of the H$^+$ catalyzed CA reactions of H$^+$: imine complex **4** with alkene 1 indicates that this CA reaction takes place through a stepwise mechanism [65,66]. Therefore, for each reactive path, we studied one possible CA with two transition states and one intermediate (see Scheme 5). The structure of the transition states corresponding to this CA reaction as well as the lengths of the new bonds are shown in Figure 5. The total energies have been collected in Table S3 in Supplementary Material, and relative ones are inserted in Scheme 5. The gas phase energy profiles of all possible reactive paths are given in Figure 6.

Scheme 5. The pathways involved in the Povarov reaction of alkene **1** with H⁺:imine complex **4** together with the relative energies (in kcal/mol), red refers to the reagents and blue refers to the molecular complex.

We can notice that by considering the sum of the reagent energies as a reference, the activation energies of all competitive pathways are negative (red values in Scheme 5), and if we consider the formation of a molecular complex (MC) in the first stage of the reaction as a reference, these activation energies become positive (blue values in Scheme 5). Firstly, by a comparison between the activation energies of the first and the second steps, we can notice that the first step is the rate-determining step for the meta regioisomeric reactive paths. Secondly, from a comparison between the activation energies of the first step of this cycloaddition, we notice that the meta regioisomeric pathways are more favored than the ortho ones by around 4 kcal/mol, which accounts for a complete regioselectivity of these pathways. Therefore, the Brønsted catalysed reaction between imine:H⁺ complex **4** and alkene **1** leading to the formation of the corresponding meta regioisomers is in agreement with local reactivity indices analysis and experimental finding. On the other hand, we can notice that the obtained cycloadducts are less stable than the corresponding intermediates, which accounts for the reversibility of this cycloaddition, which explain well the obtained moderate yield.
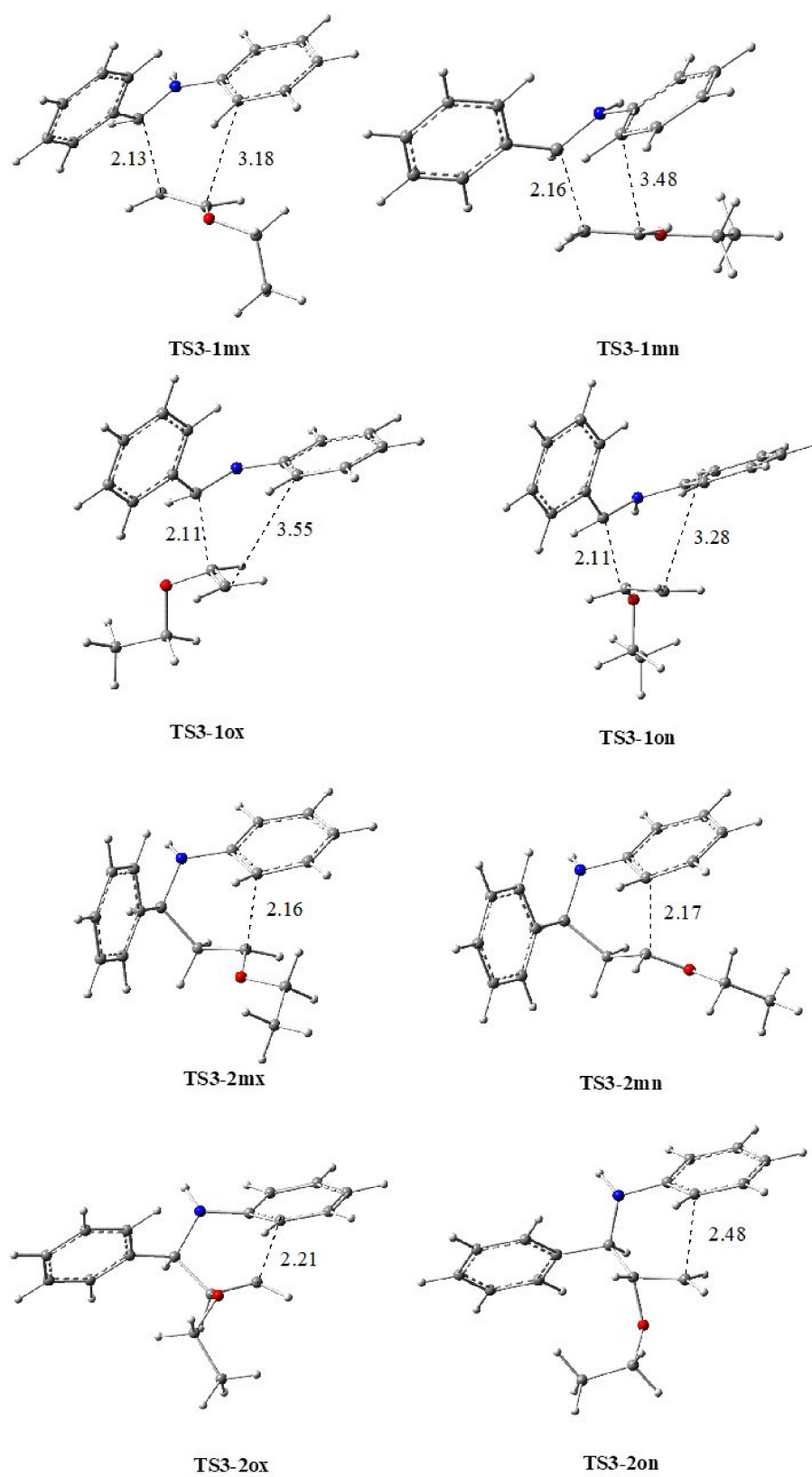
Figure 5. Optimized structures of the TSs associated with the Brønsted catalyzed reaction between imine:H$^+$ complex **4** and alkene **1**, together with lengths of the new forming bonds.
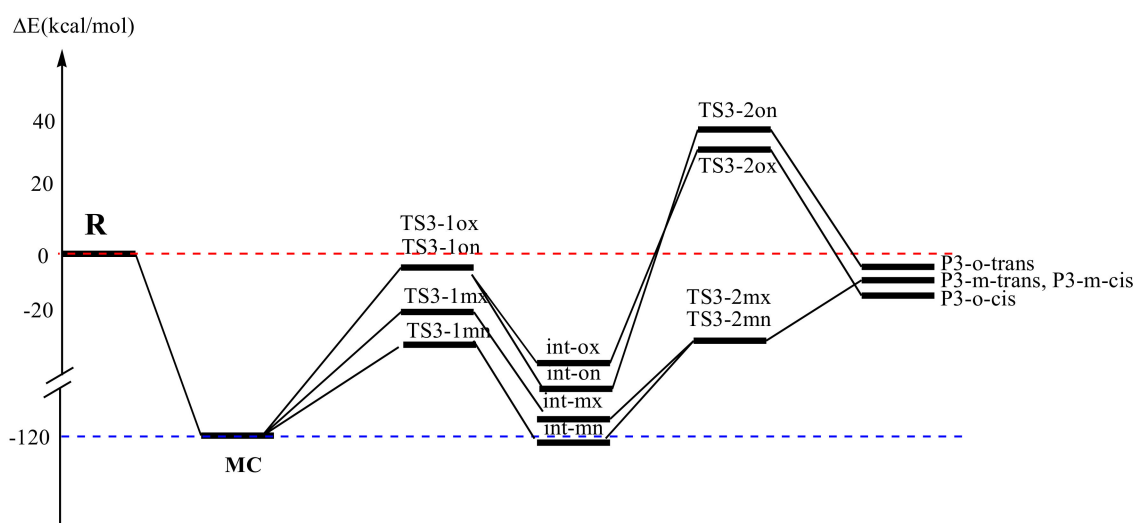
Figure 6. Energy profiles for the Brønsted catalyzed reaction between imine:H$^+$ complex **4** and alkene **1**.

By a comparison between the activation energy of the more favored approach of the first step **TS3-1mn** (17.19 kcal/mol) and that with the use of AlCl$_3$ catalysis, **TS2-mn** (14.39 kcal/mol), we conclude that the AlCl$_3$ is the best catalyst of this reaction type, which is in agreement with experimental data.

3. Conclusions

In this work, we have performed an experimental as well as a theoretical investigation of the role of the catalyst in the Povarov cycloaddition reaction of imine(derived from benzaldehyde and aniline) with different substituted alkenes.

In the experimental part, we have synthesized a quinoline derivative **5** using the Povarov method between an imine and substituted alkenes, in the absence and in the presence of a catalyst through two methods.

In the first method, we prepared the meta regioisomer of quinoline **5** with a good yield from the previously prepared imine (from aniline with benzaldehyde) and its reaction with alkene (methyl-vinyl-ether) in the presence of a Lewis acid catalyst and obtained a high yield, while this reaction did not occur with the use of allyl alcohol as alkene.

In the second method, we used a multi-component reaction between aniline, benzaldehyde, and alkene **1** at the same time, in the presence of a Brønsted acid catalyst, namely acetic acid or hydrochloric acid, leading to the meta regioisomer of quinoline derivative **5** with a moderate yield. The quinoline derivative **5** which has been obtained by both methods has the same physicochemical properties, in which its structure has been confirmed by the usual spectroscopic methods. This reaction does not take place when the catalyst is not added or if allyl alcohol is used as alkene. The biological activity of the prepared quinoline derivative **5** has been evaluated against six types of bacteria, in which the obtained results reveal that this product hasin vitroantibacterial activity against both *Escherichia coli* and *Staphylococcus aureus*. This product has been also used for possible antioxidant activity, which indicates a high reactivity with the DPPH radical.

In the theoretical part, we performed a computational study of the mechanism and the selectivity of the cycloaddition step in the Povarov reaction between imine **2** and vinyl ethyl ether or allyl alcohol using DFT methods at the B3LYP/6-31G(d,p) theoretical level. The main conclusions that can be extracted from our results are the following:

Analysis of the CDFT reactivity indices at the ground state of the reagents involved in these cycloaddition reactions indicates that imine **2** is a moderate electrophile. Coordination of Lewis or Brønsted acid to the imine **2** increases its electrophilicity, leading to enhancing its reactivity toward electron-rich alkenes such as alkene **1**. The ethyl vinyl ether reacts as a strong nucleophile, whereas alkene allyl alcohol reacts as a marginal nucleophile, which needs high activation energy to react with imines.

The analysis of local reactivity indices based on the Parr functions method predicts correctly the meta regioselectivity observed experimentally.

The cycloaddition step between imine **2** and alkene **1** in the absence of a catalyst proceedsviaa relatively asynchronous non-polar mechanism leading to the formation of meta regioisomers by high activation energies.

In the presence of a Lewis acid such as AlCl$_3$, the activation energies decrease dramatically, justifying the high obtained experimental yield. This cycloaddition step favors the formation of meta regioisomers through a highly asynchronous polar mechanism.

In the presence of Brønsted acid, the obtained activation energies are lower than that without catalyst and higher than that obtained with the used Lewis acid catalyst, justifying the obtained moderate yield. This cycloaddition reaction proceeds through a stepwise mechanism in which the first step is the rate-determining step, favoring the formation of meta regioisomers. The obtained results reveal that this reaction is a reversible process justifying the moderate and low yield obtained experimentally.

Supplementary Materials: Supplementary materials are available online at https://www.mdpi.com/2673-401X/2/1/6/s1.

Author Contributions: Conceptualization, A.K.N.; methodology, A.K.N.; software, A.K.N.; validation, S.L., A.H. and M.K.; formal analysis, A.K.N., S.L., A.H. and M.K.; investigation, A.K.N., S.L., A.H., M.K. and W.Y.; resources, A.K.N.; data curation, A.K.N., S.L., A.H. and M.K.; writing—original draft preparation, A.K.N.; writing—review and editing, A.K.N.; visualization, A.K.N.; supervision, A.K.N.; project administration, A.K.N.; funding acquisition, A.K.N. All authors have read and agreed to the published version of the manuscript.

Institutional Review Board Statement: Not applicable.

Informed Consent Statement: Not applicable.

Data Availability Statement: Data is contained within supplementary material.

Conflicts of Interest: The authors declare no conflict of interest.

References

1. Vo, C.-V.T.; Bode, J.W. Synthesis of Saturated N-Heterocycles. *J. Org. Chem.* **2014**, *79*, 2809–2815. [CrossRef]
2. Paoletti, P.; Neyton, J. NMDA receptor subunits: Function and pharmacology. *Curr. Opin. Pharmacol.* **2007**, *7*, 39–47. [CrossRef] [PubMed]
3. Rano, T.A.; Sieber-McMaster, E.; Pelton, P.D.; Yang, M.; Demarest, K.T.; Kuo, G.-H. Design and synthesis of potent inhibitors of cholesteryl ester transfer protein (CETP) exploiting a 1,2,3,4-tetrahydroquinoline platform. *Bioorg. Med. Chem. Lett.* **2009**, *19*, 2456–2460. [CrossRef] [PubMed]
4. Ramesh, C.; Nayak, T.K.; Burai, R.; Dennis, M.K.; Hathaway, H.J.; Sklar, L.A.; Prossnitz, E.R.; Arterburn, J.B. Synthesis and cha-racterization of iodinated tetrahydroquinolines targeting the G protein-coupled estrogen receptor GPR30. *J. Med. Chem.* **2010**, *53*, 1004–1014. [CrossRef]
5. Caprio, V.; Guyen, B.; Opoku-Boahen, Y.; Mann, J.; Gowan, S.M.; Kelland, L.M.; Read, M.A.; Neidle, S. A novel inhibitor of human telomerase derived from 10H-indolo [3, 2-b] quinoline. *Bioorg. Med. Chem. Lett.* **2000**, *10*, 2063–2066. [CrossRef]
6. Senthilkumar, P.; Dinakaran, M.; Yogeeswari, P.; Sriram, D.; China, A.; Nagaraja, V. Synthesis and antimycobacterial activities of novel 6-nitroquinolone-3-carboxylic acids. *Eur. J. Med. Chem.* **2009**, *44*, 345–358. [CrossRef] [PubMed]
7. Delgado, J.; Wilson, R.W. *Gisvold's Textbook of Organic Medicinal and Pharmaceutical Chemistry*; Lippinicott Williams and Wilkins: Philadelphia, PA, USA, 1998; Volume 185.
8. Guo, L.-J.; Wei, C.-X.; Jia, J.-H.; Zhao, L.-M.; Quan, Z.-S. Design and synthesis of 5-alkoxy-[1, 2, 4] triazolo [4, 3-a] quinoline derivatives with anticonvulsant activity. *Eur. J. Med. Chem.* **2009**, *44*, 954–958. [CrossRef]
9. Clemence, F.; Le Martret, O.; Delevallee, F.; Benzoni, J.; Jouanen, A.; Jouquey, S.; Mouren, M.; Deraedt, R. 4-Hydroxy-3-quinolinecarboxamides with antiarthritic and analgesic activities. *J. Med. Chem.* **1988**, *31*, 1453–1462. [CrossRef]
10. Sircar, I.; Haleen, S.J.; Burke, S.E.; Barth, H. Synthesis and biological activity of 4-(diphenylmethyl)-alpha-[(4-quinolinyloxy)methyl]-1-piperazineethanol and related compounds. *J. Med. Chem.* **1992**, *35*, 4442–4449. [CrossRef]

11. Kouznetsov, V.V. Recent synthetic developments in a powerful imino Diels-Alder reaction (Povarov reaction): Application to the synthesis of N-polyheterocycles and related alkaloids. *Tetrahedron* **2009**, *65*, 2721–2750. [CrossRef]

12. Katritzky, A.R.; Rachwal, S.; Rachwal, B. Recent progress in the synthesis of 1, 2, 3, 4,-tetrahydroquinolines. *Tetrahedron* **1996**, *52*, 15031–15070. [CrossRef]

13. Oikawa, H.; Tokiwano, T. Enzymatic catalysis of the Diels-Alder reaction in the biosynthesis of natural products. *Nat. Prod. Rep.* **2004**, *21*, 321–352. [CrossRef]

14. Lucchini, V.; Prato, M.; Scorrano, G.; Stivanello, M.; Valle, G. Acid-catalysed addition of N-aryl imines to dihydrofuran. Postulated dependence of the reaction mechanism on the relative face of approach of reactants. *J. Chem. Soc. Perkin Trans.* **1992**, *2*, 259–266. [CrossRef]

15. Makioka, Y.; Shindo, T.; Taniguchi, Y.; Takaki, K.; Fujiwara, Y. Ytterbium (III) triflate catalyzed synthesis of quinoline derivatives from N-arylaldimines and vinyl ethers. *Synthesis* **1995**, *1995*, 801–804. [CrossRef]

16. Liu, R.H.; Yu, X.; Hu, L.; Yu, N.F. Simple and practical synthesis of pyrano- and furano[3,2-c]-quinoline derivatives under non-Lewis acid catalysis. *Chin. Chem. Lett.* **2012**, *23*, 1027–1030. [CrossRef]

17. Povarov, L.S. αβ-Unsaturated ethers and their analogues in reactions of diene synthesis. *Russ. Chem. Rev.* **1967**, *36*, 656–670. [CrossRef]

18. Grieco, P.A.; Bahsas, A. Role reversal in the cyclocondensation of cyclopentadiene with heterodienophiles derived from aryl amines and aldehydes: Synthesis of novel tetrahydroquinolines. *Tetrahedron Lett.* **1988**, *29*, 5855–5858. [CrossRef]

19. Kobayashi, S.; Nagayama, S. A New Methodology for Combinatorial Synthesis. Preparation of Diverse Quinoline Derivatives Using a Novel Polymer-Supported Scandium Catalyst. *J. Am. Chem. Soc.* **1996**, *118*, 8977–8978. [CrossRef]

20. Ma, Y.; Qian, C.; Xie, M.; Sun, J. Lanthanide Chloride Catalyzed Imino Diels-Alder Reaction. One-Pot Synthesis of Pyrano [3, 2-c]-and Furo [3, 2-c] quinolines. *J. Org. Chem.* **1999**, *64*, 6462–6467. [CrossRef]

21. Lavilla, R.; Bernabeu, M.C.; Carranco, I.; Díaz, J.L. Dihydropyridine-based multicomponent reactions. Efficient entry into new tetrahydroquinoline systems through Lewis acid-catalyzed formal [4+ 2] cycloadditions. *Org. Lett.* **2003**, *5*, 717–720. [CrossRef] [PubMed]

22. Powell, D.A.; Batey, R.A. Lanthanide(III)-catalyzed multi-component aza-Diels-Alder reaction of aliphatic N-arylaldimines with cyclopentadiene. *Tetrahedron Lett.* **2003**, *44*, 7569–7573. [CrossRef]

23. Batey, R.A.; Powell, D.A. Multi-component coupling reactions: Synthesis of a guanidine containing analog of the hexahydro-pyrrolo [3, 2-c] quinoline alkaloid martinelline. *Chem. Commun.* **2001**, *22*, 2362–2363. [CrossRef]

24. Yadav, J.S.; Reddy, B.V.S.; Srinivas, R.; Madhuri, C.; Ramalingam, T. Lithium perchlorate/diethylether catalyzed aza-Diels-Alder reaction: An expeditious synthesis of pyrano, indeno quinolines and phenanthridines. *Synlett* **2001**, *2001*, 240–242. [CrossRef]

25. Legros, J.; Crousse, B.; Ourevitch, M.; Bonnet-Delpon, D. Facile synthesis of tetrahydroquinolines and julolidines through mul-ticomponent reaction. *Synlett* **2006**, *2006*, 1899–1902. [CrossRef]

26. Nacereddine, A.K.; Layeb, H.; Chafaa, F.; Yahia, W.; Djerourou, A.; Domingo, L.R. A DFT study of the role of the Lewis acid catalysts in the [3 + 2] cycloaddition reaction of the electrophilic nitrone isomer of methyl glyoxylate oxime with nucleophilic cyclopentene. *RSC Adv.* **2015**, *5*, 64098–64105. [CrossRef]

27. Barama, L.; Bayoud, B.; Chafaa, F.; Nacereddine, A.K.; Djerourou, A. A mechanistic MEDT study of the competitive catalysed [4+2] and [2+2] cycloaddition reactions between 1-methyl-1-phenylallene and methyl acrylate: The role of Lewis acid on the mechanism and selectivity. *Struct. Chem.* **2018**, *29*, 1709–1721. [CrossRef]

28. Bouacha, S.; Nacereddine, A.K.; Djerourou, A. A theoretical study of the mechanism, stereoselectivity and Lewis acid catalyst on the Diels-Alder cycloaddition between furan and activated alkenes. *Tetrahedron Lett.* **2013**, *54*, 4030–4033. [CrossRef]

29. Yahia, W.; Nacereddine, A.K.; Liacha, M. Towards Understanding the Role of Lewis Acid on the Regioselectivity and Mechanism for the Acetylation Reaction of 2-benzoxazolinone with Acetyl Chloride: A DFT Study. *Prog. React. Kinet. Mech.* **2014**, *39*, 365–374. [CrossRef]

30. Lachtar, Z.; Nacereddine, A.K. Understanding the origin of the enantioselectivity and the mechanism of the asymmetric re-duction of ketimine generated from acetophenone with oxazaborolidine catalyst. *Struct. Chem.* **2020**, *31*, 253–261. [CrossRef]

31. Eyring, H. The Activated Complex in Chemical Reactions. *J. Chem. Phys.* **1935**, *3*, 107–115. [CrossRef]

32. Geerlings, P.; De Proft, A.F.; Langenaeker, W. Conceptual Density Functional Theory. *Chem. Rev.* **2003**, *103*, 1793–1874. [CrossRef] [PubMed]

33. Domingo, L.R.; Ríos-Gutiérrez, M.; Pérez, P. Applications of the conceptual density functional theory indices to organic che-mistry reactivity. *Molecules* **2016**, *21*, 748. [CrossRef]

34. Gawroński, J.; Wascinska, N.; Gajewy, J. Recent Progress in Lewis Base Activation and Control of Stereoselectivity in the Additions of Trimethylsilyl Nucleophiles. *Chem. Rev.* **2008**, *108*, 5227–5252. [CrossRef]

35. Nic, M.; Hovorka, L.; Jirat, J.; Kosata, B.; Znamenacek, J. *IUPAC Compendium of Chemical Terminology—The Gold Book*; International Union of Pure and Applied Chemistry: Research Triangle Park, NC, USA, 2005.

36. Schiff, H. Eine Reihe. *Eur. J. Org. Chem.* **1864**, *131*, 118–119.

37. Layer, R.W. The Chemistry of Imines. *Chem. Rev.* **1963**, *63*, 489–510. [CrossRef]

38. Posson, H.; Hurvois, J.-P.; Moinet, C. Imino Diels-Alder Reaction: Application to the Synthesis of Diverse Cyclopenta[c]Quinoline Derivatives. *Synlett* **2000**, *2000*, 209–212. [CrossRef]

39. Kiselyov, A.S.; Smith, L.; Virgilio, A.; Armstrong, R.W. Immobilized aldehydes and olefins in the solid support synthesis of tetrahydroquinolines via a three component condensation. *Tetrahedron* **1998**, *54*, 7987–7996. [CrossRef]

40. Seeley, H.W., Jr.; Van Demark, P.J. *Microbes in Action. A Laboratory Manual of Microbiology*; W. H. Freeman & Co.: San Francisco, CA, USA; London, UK, 1962.

41. Di Meo, F.; Lemaur, V.; Cornil, J.; Lazzaroni, R.; Duroux, J.-L.; Olivier, Y.; Trouillas, P. Free radical scavenging by natural po-lyphenols: Atom versus electron transfer. *J. Phys. Chem. A* **2013**, *117*, 2082–2092. [CrossRef]

42. Salah, N.; Miller, N.; Paganga, G.; Tijburg, L.; Bolwell, G.; Riceevans, C. Polyphenolic Flavanols as Scavengers of Aqueous Phase Radicals and as Chain-Breaking Antioxidants. *Arch. Biochem. Biophys.* **1995**, *322*, 339–346. [CrossRef]

43. Blois, M.S. Antioxidant Determinations by the Use of a Stable Free Radical. *Nature* **1958**, *181*, 1199–1200. [CrossRef]

44. Frisch, M.J.; Trucks, G.W.; Schlegel, H.B.; Scuseria, G.E.; Robb, M.A.; Cheeseman, J.R.; Scalmani, G.; Barone, V.; Petersson, G.A.; Nakatsuji, H.; et al. *Gaussian09*; Gaussian Inc.: Wallingford, CT, USA, 2010.

45. Becke, A.D. Density-functional exchange-energy approximation with correct asymptotic behavior. *Phys. Rev. A* **1988**, *38*, 3098. [CrossRef] [PubMed]

46. Becke, A.D. A new mixing of Hartree-Fock and local density functional in atoms molecules and solids by the spin-density-functional formalism. *Phys. Rev.* **1988**, *38*, 3098–3100. [CrossRef] [PubMed]

47. Lee, C.; Yang, W.; Parr, R.G. Development of the Colle-Salvetti correlation-energy formula into a functional of the electron density. *Phys. Rev. B* **1988**, *37*, 785–789. [CrossRef] [PubMed]

48. Reed, A.E.; Curtiss, L.A.; Weinhold, F. Intermolecular interactions from a natural bond orbital, donor-acceptor viewpoint. *Chem. Rev.* **1988**, *88*, 899–926. [CrossRef]

49. Parr, R.G.; Szentpály, L.V.; Liu, S. Electrophilicity Index. *J. Am. Chem. Soc.* **1999**, *121*, 1922–1924. [CrossRef]

50. Parr, R.G.; Pearson, R.G. Absolute hardness: Companion parameter to absolute electronegativity. *J. Am. Chem. Soc.* **1983**, *105*, 7512–7516. [CrossRef]

51. Domingo, L.R.; Chamorro, E.; PérezP, P. Understanding the Reactivity of Captodative Ethylenes in Polar Cycloaddition Reactions. A Theoretical Study. *J. Org. Chem.* **2008**, *73*, 4615–4624. [CrossRef] [PubMed]

52. Kohn, W.; Sham, L.J. Self-Consistent Equations Including Exchange and Correlation Effects. *Phys. Rev.* **1965**, *140*, A1133. [CrossRef]

53. Domingo, L.R.; Pérez, P.; Sáez, J.A. Understanding the local reactivity in polar organic reactions through electrophilic and nucleophilic Parr functions. *RSC Adv.* **2013**, *3*, 1486–1494. [CrossRef]

54. Domingo, L.R. A new C–C bond formation model based on the quantum chemical topology of electron density. *RSC Adv.* **2014**, *4*, 32415–32428. [CrossRef]

55. Ríos-Gutiérrez, M.; Chafaa, F.; Nacereddine, A.K.; Djerourou, A.; Domingo, L.R. A DFT study of [3 + 2] cycloaddition reactions of an azomethine imine with N-vinyl pyrrole and N-vinyl tetrahydroindole. *J. Mol. Graph. Model.* **2016**, *70*, 296–304. [CrossRef] [PubMed]

56. Nacereddine, A.K.; Yahia, W.; Sobhi, C.; Djerourou, A. A theoretical study of the mechanism and stereoselectivity of the Diels–Alder cycloaddition between difluoro-2-methylencyclopropane and furan. *Tetrahedron Lett.* **2012**, *53*, 5784–5786. [CrossRef]

57. Hellel, D.; Chafaa, F.; Nacereddine, A.K.; Djerourou, A.; Vrancken, E. Regio- and stereoselective synthesis of novel isoxazolidine heterocycles by 1,3-dipolar cycloaddition between C-phenyl-N-methylnitrone and substituted alkenes. Experimental and DFT investigation of selectivity and mechanism. *RSC Adv.* **2017**, *7*, 30128–30141. [CrossRef]

58. Bayoud, B.; Barama, L.; Nacereddine, A.K.; Djerourou, A. Shedding light on the factors controlling the mechanism, selectivity and reactivity of the Diels-Alder reactions between substituted pyridinones and ethylenes: A MEDT study. *Mol. Phys.* **2021**, *119*, e1828635. [CrossRef]

59. Nacereddine, A.K. A MEDT computational study of the mechanism, reactivity and selectivity of non-polar [3+2] cycloaddition between quinazoline-3-oxide and methyl 3-methoxyacrylate. *J. Mol. Model.* **2020**, *26*, 328. [CrossRef]

60. Chermette, H. Chemical reactivity indexes in density functional theory. *J. Comput. Chem.* **1999**, *20*, 129–154. [CrossRef]

61. Domingo, L.R.; Aurell, M.; Pérez, P.; Contreras, R. Quantitative characterization of the global electrophilicity power of common diene/dienophile pairs in Diels-Alder reactions. *Tetrahedron* **2002**, *58*, 4417–4423. [CrossRef]

62. Jaramillo, P.; Domingo, L.R.; Chamorro, E.; Pérez, P. A further exploration of a nucleophilicity index based on the gas-phase ionization potentials. *J. Mol. Struct. Theochem.* **2008**, *865*, 68–72. [CrossRef]

63. Domingo, L.R.; Pérez, P.; Sáez, J.A. Origin of the synchronicity in bond formation in polar Diels-Alder reactions: An ELF analysis of the reaction between cyclopentadiene and tetracyanoethylene. *Org. Biomol. Chem.* **2012**, *10*, 3841–3851. [CrossRef] [PubMed]

64. Domingo, L.R.; Aurell, M.J.; Pérez, P. A DFT analysis of the participation of zwitterionic TACs in polar [3+2] cycloaddition reactions. *Tetrahedron* **2014**, *70*, 4519–4525. [CrossRef]

65. Jasiński, R. First example of stepwise, zwitterionic mechanism for bicyclo [2.2. 1] hept-5-ene (norbornene) formation process catalyzed by the 1-butyl-3-methylimidazolium cations. *Monatshefte Chem. Chem. Mon.* **2016**, *147*, 1207–1213. [CrossRef] [PubMed]

66. Domingo, L.R.; Aurell, M.J.; Pérez, P. The mechanism of ionic Diels-Alder reactions. A DFT study of the oxa-Povarov reaction. *RSC Adv.* **2014**, *4*, 16567–16577. [CrossRef]